Calcif Tissue Int (2001) 68:192–201
DOI: 10.1007/s002230010015

Calcified Tissue International

Junctional Proteins and Ca^{2+} Transport in the Rat Odontoblast-Like Cell Line MRPC-1

T. Lundgren,[1] M. Nilsson,[2] H. H. Ritchie,[3] A. Linde[1]

[1]Department of Oral Biochemistry, Göteborg University, Göteborg, Sweden
[2]Institute of Anatomy & Cell Biology, Göteborg University, Göteborg, Sweden
[3]Department of Cariology, Restorative Science & Endodontics, School of Dentistry, University of Michigan, Ann Arbor, Michigan MI, USA

Received: 28 August 2000 / Accepted: 1 December 2000 / Online publication: 13 March 2001

Abstract. A transcellular bulk flow of Ca^{2+} ions through the odontoblast layer is of central importance during dentinogenesis. For this, specialized mechanisms may exist, which by a concerted action, gate Ca^{2+} into the proximal end of the cells and extrude the ions towards the mineralization front. To elucidate these mechanisms, an *in vitro* model would be useful. Mature odontoblasts are, however, post-mitotic cells and cannot be propagated in cell culture. The aim of the present study was, therefore, to characterize the odontoblast-like rat cell line MRPC-1[1] with regard to transcellular Ca^{2+} transport, barrier function, and intercellular junctions when cultured on membranes in Transwell chambers. The MRPC-1 cells grew as epithelial-like cells in a continuous bilayer separated by a thin collagenous matrix and with intercellular junctional complexes. They exhibited properties of a low-resistance epithelium, maintained a Ca^{2+}-dependent diffusion barrier, and exhibited a functional diversity between the two cell layers. MRPC-1 cells expressed ZO-1, occludin, E-, and N-cadherins in addition to α-, β-, γ- and $p120^{cat}$ catenins, thereby demonstrating some traits in common with, but also differences from, epithelial cells and major differences from fibroblasts. The transcellular Ca^{2+} flux was inhibitable by nifedipine unidirectionally, giving evidence for an active intracellular Ca^{2+} transport through voltage-gated channels of the L-type. Similarities with native odontoblasts indicate that MRPC-1 cells may be useful for *in vitro* studies of transcellular Ca^{2+} transport mechanisms of importance for the calcification process.

Key words: Calcification — Dentinogenesis — Cadherins — Catenins — Intercellular junctions

Odontoblasts are ectomesenchymal cells of neural crest cell origin. They play a central role during the formation of dentin by synthesizing collagen and noncollagenous macromolecules of the dentin organic matrix [1]. In addition, the odontoblasts are instrumental in mineral formation [2]. As for the closely related osteogenesis, a transcellular bulk flow of Ca^{2+} ions takes place, and earlier studies indicate that this occurs primarily by an intracellular route, *i.e.*, through the odontoblasts [3–5]. The Ca^{2+} activity in predentin, *i.e.*, just in advance of the mineralization front, is 2–3 times higher than that at the proximal (pulpal) side of the odontoblasts [5], suggesting that odontoblasts constitute a diffusion barrier between the two compartments, and Ca^{2+} ions are actively transported in a controlled and directed manner. For this transport, specialized mechanisms may exist in odontoblasts, which by a concerted action, gate Ca^{2+} into the proximal end of the cells and extrude the ions at their distal end towards the site of mineral formation [2, 4, 6, 7].

As Ca^{2+} transport is of importance for dentinogenesis, it would be advantageous to obtain an *in vitro* experimental model, in which Ca^{2+} fluxes can be studied and quantified, and Ca^{2+} transport mechanisms and their regulation can be further elucidated in detail. Mature dentinogenic odontoblasts are, however, post-mitotic cells and cannot be propagated in cell culture, and few convincing odontoblast-like cell lines have hitherto been published. The novel cell line MRPC-1[1], an *in vitro* mineralizing subclone of the dental pulp cell line RPC-C2A [8], exhibits an odontoblast-like phenotype. Specifically, the cells express dentin-specific dentin sialophosphoprotein (DSPP), collagen type I, high alkaline phosphatase activity [M. Marsh & H. H. Ritchie, unpublished] and the three isoforms of the NCX1 Na^+/Ca^{2+} exchanger, NaCa 3, 7, and 10, characteristic of native odontoblasts and osteoblastic cells [9].

The aim of the present study was, therefore, to characterize the odontoblast-like cell line MRPC-1, cultured in Transwell inserts, with respect to barrier function, expression of different tight and adherens junction proteins, and transcellular Ca^{2+} transport. The results show that MRPC-1 cells, indeed, maintain a barrier function, display intercellular junctional complexes, and perform an active and inhibitable transport of Ca^{2+} ions, making MRPC-1 cells an interesting model for transcellular Ca^{2+} transport studies *in*

Correspondence to: T. Lundgren
[1] *The MRPC-1 cell line was previously denoted MMP4.*

vitro. This may be of importance for a further understanding of the detailed mechanisms involved in the calcification process, specifically dentinogenesis.

Materials and Methods

Chemicals

α-MEM, fetal bovine serum, penicillin, streptomycin, L-glutamine, fungizone, ascorbic acid, and all other cell culture components were obtained from Gibco BRL Life Technologies (Roskilde, Denmark). Nifedipine was obtained from Sigma Chemical Co. (St. Louis, MO, USA). A stock solution of nifedipine (1 mM) in DMSO was prepared and stored in light-safe boxes. $^{45}CaCl_2$ was obtained from ICN Biomedicals (Costa Mesa, CA, USA). Primary antibodies directed against human ZO-1 (zonula occludens-1), occludin, and N-cadherin were obtained from Zymed Laboratories (San Francisco, CA, USA). Pan-cadherin antibodies were obtained from Sigma, and antibodies to human E-cadherin and murine α-, β-, γ(plakoglobin)- and $p120^{cat}$ catenins were from Transduction Laboratories (Lexington, KY, USA).

Cell Culture

Rat odontoblast-like MRPC-1 cells were seeded in either Lab-Tek Culture chamber slides (Nunc, Naperville, IL, USA) or in 6.5 mm Transwells (Costar, Badhoevedorp, Netherlands) in α-MEM (minimum essential medium) with additions of 10% fetal bovine serum, 100 U/ml penicillin, 100 μg/ml streptomycin, 2 mM L-glutamine, 1% fungizone, 50 μg/ml ascorbic acid, and 1.8 mM $CaCl_2$ at 37°C in a 5% CO_2 atmosphere. Medium was changed every 2nd day. Typically, cells were kept in culture for 6–8 days before use. The lower and upper media volumes in the bicameral Transwells were 500 and 200 μl, respectively. Porcine thyrocytes, isolated as previously described [10] were cultured in 6.5 mm Transwells in α-MEM with the addition of 5% fetal calf serum, 200 U/ml penicillin, 200 μg/ml streptavidin, and 2.5 μg/ml fungizone at 37°C in a 5% CO_2 atmosphere. Confluent monolayers were formed after 4–5 days. Madin-Darby canine kidney (MDCK) cells and MRC-5 fibroblasts were cultured as described [11]

Transmission Electron Microscopy

Filter-cultured MRPC-1 cells were fixed with 2.5% glutaraldehyde in sodium cacodylate buffer for 1 hour. After rinsing twice in sodium cacodylate buffer, the cells were postfixed in 1% OsO_4 for 1 hour, after which the Transwell membranes were cut out of the inserts and dehydrated in ascending grades of ethanol. After embedding in epoxy resin, perpendicular sections were contrasted with uranyl acetate and examined in a Philips 400 transmission electron microscope.

Immunofluorescence

After fixation in ice-cold ethanol for 20 minutes and preincubation for 5 minutes in phosphate-buffered saline containing 7.5% sucrose, 5% fat-free milk, and 0.1% gelatin, MRPC-1 cells cultured in Lab-Tek Culture chamber slides were incubated with primary ZO-1, occludin, E-cadherin, pan-cadherin, or β-catenin antibodies, followed by biotin-labeled IgG and FITC-streptavidin. Each incubation lasted for 30 minutes followed by 3 × 5 minute washings. Examination and photography was performed with a Nikon FXA fluorescence microscope on Kodak T-max 400 ISO film.

Western Blotting

Confluent MRPC-1 cells, MDCK cells, pig thyrocytes, and MRC-5 fibroblasts were boiled for 4 minutes in sample buffer with 5% mercaptoethanol. Samples with equal amounts of protein were resolved by SDS-PAGE on 4–15% gradient gels, and transferred to 0.45 μm nitrocellulose sheets in a Bio-Rad mini-trans-blot cell (Bio-Rad Laboratories, Hercules, CA, USA). The blotted sheets were washed in Tris-buffered saline with 5% fat-free dry milk and 0.1% Tween followed by sequential 1-hour incubations with primary and horseradish peroxidase-conjugated secondary antibodies, respectively. After washing 6 × 5 minutes in Tris-buffered saline, immunoreactivity was detected by Enhanced ChemiLuminiscence (Amersham) and visualized by exposure to X-ray film. As a reference, prestained molecular weight standards (Bio-Rad) were used.

Paracellular Electrical Resistance

The paracellular electrical resistance across cell layers cultured on the Transwell filters was measured by a Millicell ERS Ω-meter (Millipore, Bedford, MA, USA) at 1, 3, 6, and 8 days after seeding, and bare filter resistance was subtracted from the test measurements.

Transcellular Ca^{2+} Flux

MRPC-1 cells and pig thyrocytes cultured in Transwell chambers were incubated in the presence or absence (Ca^{2+}-free Hanks medium + 0.5 mM EGTA) of Ca^{2+} in either of the lower or upper chambers. In the isotope-containing chamber, Ca^{2+}-free Hanks medium was used without EGTA. $^{45}Ca^{2+}$ (final activity 0.01 μCi/ml) was added to either the lower or the upper chamber. After 5, 10, 15, or 20 minutes, respectively, the liquid in the non-isotope-containing chamber was collected. From these aliquots, liquid scintillation samples were prepared and measured in an LKB Wallac 1215 Rackbeta liquid scintillation counter.

Results are presented as means ± SD. Statistical analyses were performed using a computerized unpaired Student's *t*-test (StatView 4.01). $P < 0.05$ was considered to demonstrate a significant difference.

Results

Paracellular Electrical Resistance

Confluent MRPC-1 cells grown on Transwell filters in Ca^{2+}-containing medium established a low paracellular resistance of $<200\ \Omega \cdot cm^2$. One day after seeding, resistance differed significantly from the bare transfilter resistance ($P < 0.001$) (Fig. 1). After 3 days of culture, the transcellular resistance essentially reached a plateau, and from day 6 on the the values no longer increased (not shown).

Transmission Electron Microscopy

When cultured for 6 days in Ca^{2+}-containing α-MEM, MRPC-1 cells were arranged on the Transwell filters as two continuous layers of flattened cells separated by a narrow space (Fig. 2A). The cytoplasm of all cells had a flat elongated nucleus with poor morphological polarization in terms of nuclear localization (Fig. 2A). Junctional complexes were seen in the intercellular spaces of the superior cell layer. The cell height of the superior cell layer was somewhat greater than the inferior, and occasionally villi-like cytoplasmic extensions were observed along its cell surface

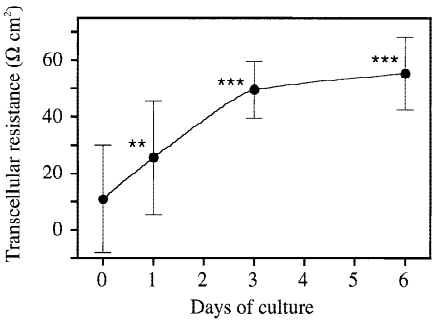

Fig. 1. MRPC-1 cells grown on Transwell membranes in Ca^{2+}-containing medium formed low transcellular resistance (<200 Ω · cm^2) cell layers. From day 1 after seeding, the resistance already differed significantly from the bare transmembrane resistance ($P < 0.001$). At day 6 after seeding, the transcellular resistance reached a maximal value.

(Fig. 2B). The cytoplasm of both cell layers contained numerous mitochondria along with rough endoplasmic reticulum. The basal cell layer tended to lie directly on the Transwell filter with no discernible matrix between cells and filter (Fig. 2C). Between the cell layers, a collagenous matrix with regular outlines was present. The collagen fibers were arranged in parallel with the flat cells (Fig. 2D).

Immunofluorescence

Immunofluorescent staining of MRPC-1 cells cultured for 6–8 days exhibited a polygonal cellular outline and revealed a difference between the upper and lower cell layers as to the distribution of cell adhesion molecules (Fig. 3). ZO-1 immunoreactivity of the upper cell layer appeared as thin homogenous lines along the circumference of all cells (Fig. 3A). Below the upper cell layer the homogenous ZO-1 immunoreactivity was lost, the staining appearing as irregular dots with no continuity (Fig. 3B). In the same way, E-cadherin immunoreactivity of the upper cell layer appeared as homogenous thin lines outlining every cell (Fig. 3C), and this immunoreactivity was lost beneath the upper cell layer (Fig. 3D). Pan-cadherin immunostaining resulted in virtually identical intensities in both the upper (Fig. 3E) and lower cell layers (not shown). The staining was continuous, outlining the circumference of the cells. In contrast, occludin immunoreactivity of the upper cell layer was irregular and weak (Fig. 3F). Within groups of cells, the staining outlined each cell, whereas other cells were essentially negative. No staining was seen in the lower cell layer (not shown). The intercellular spaces of the upper cell layer immunostained for β-catenin as thin homogenous lines around the circumference of all cells (Fig. 3G). Below the upper cell layer this regular immunoreactivity was lost, the staining appearing as irregular dots with no continuity (Fig. 3H).

Western Blotting

Immunoblotting with E-cadherin antibodies demonstrated a major band at 120 kDa in MRPC-1 cells, MDCK kidney cells and thyrocytes, whereas MRC-5 fibroblasts showed no staining for E-cadherin (Fig. 4A). The intensity was considerably lower in MRPC-1 cells compared with both MDCK cells and thyrocytes, the latter showing the highest expression. N-cadherin was immunostained as a distinct, rather strong band at 134 kDa in MRPC-1 cells, the expression being very weak in MDKC cells and MRC-5 fibroblasts, and essentially absent in thyrocytes (Fig. 4A). Pan-cadherin immunostaining revealed a major band at 134 kDa in all cell types, with the strongest staining in MRPC-1 cells and the weakest in thyrocytes (Fig. 4A).

α-catenin was expressed as a single band at 102 kDa in MRPC-1, MDKC, and thyrocytes (Fig. 4B). In MRC-5 fibroblasts the staining was barely discernible. β-catenin was expressed as a major band at 92 kDa in MRPC-1, MDKC, and thyrocytes (Fig. 4B). MRC-5 fibroblasts also exhibited β-catenin expression, although at a lower level. Staining with antibodies to γ-catenin (plakoglobin) revealed a single band at 82 kDa in MRPC-1 and MDKC cells (Fig. 4B). MRPC-1 cells showed a clearly weaker expression than both MDCK cells and thyrocytes, and in MRC-5 fibroblasts the staining was barely discernible. MRPC-1 cells, MDCK cells, and thyrocytes expressed anti-$p120^{cat}$ immunostaining (Fig. 4B). In MDKC cells a rather weak band was seen at around 100 kDa, and a clearly stronger band was revealed in thyrocytes at the same migration distance. In contrast, MRPC-1 cells showed the expression of two bands at 100 and 115 kDa, respectively, with the latter being the stronger one. In the MRC-5 fibroblasts, only the 115 kDa band was very weakly discernible.

Immunoblotting for occludin (Fig. 4C) demonstrated a strong band at 67 kDa in the MDKC cells, but MRC-5 fibroblasts expressed this band only weakly. The 67 kDa component was also present in MRPC-1 cells but, in addition, an equally strong band was seen at a higher apparent M_r. This band was also weakly seen in the other two cell types.

Transcellular Ca^{2+} Flux

MRPC-1 cells grown on Transwell membranes comprised a barrier towards $^{45}Ca^{2+}$ fluxes, when compared with cell-free Transwell membranes (Fig. 5). $^{45}Ca^{2+}$ added to the lower compartment in cell-free Transwells easily diffused into the upper compartment (Fig. 5A). When replaced with cell-covered Transwell membranes, the $^{45}Ca^{2+}$ flux was significantly ($P < 0.001$) hindered at all time points during the incubation. After 20 minutes, cell-covered Transwell membranes exhibited a 16% transcellular $^{45}Ca^{2+}$ flux as compared with cell-free Transwell membranes (Fig. 5A). When added to the upper compartment in cell-free Transwells, $^{45}Ca^{2+}$ diffused through the membrane as well (Fig. 5B). The $^{45}Ca^{2+}$ flux was significantly decreased during the 20-minute incubation when cell-free Transwell membranes

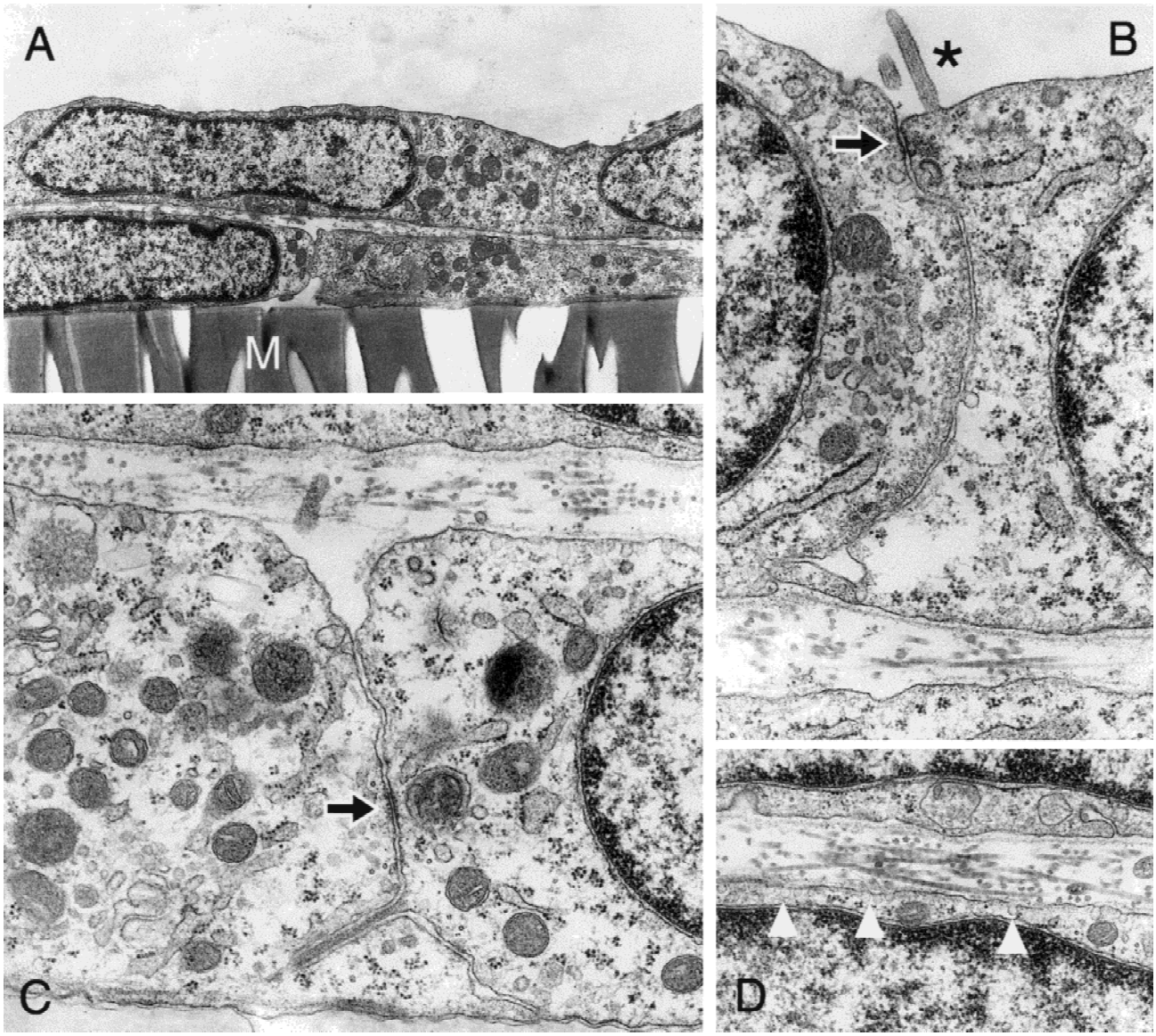

Fig. 2. Transmission electron micrographs of MRPC-1 cells. (**A**) MRPC-1 cells cultured in Ca^{2+}-containing α-MEM were arranged on the Transwell membrane (M) as a continous bi-layer of flattened cells. (**B & C**) Cells of both layers contained numerous mitochondria and rough endoplasmic reticulum. Junctional complexes (arrow in **B**) were seen in the intercellular spaces of the superior cell layer and occasionally also between the lower supporting cells (arrow in **C**). Villi-like cytoplasmic extensions (asterisk in **B**) were observed along the apical cell surface. (**D**) A thin collagenous matrix with regular outlines was present between the two cell layers with the collagen fibers parallel to the cells. Active secretion into the matrix was observed (arrowheads). (A) ×4,600; (B) ×13,000; (C) ×22,000; (D) ×17,000.

were replaced with cell-covered Transwell membranes. After 20 minutes, the MRPC-1-covered membranes exhibited 14% ($P < 0.001$) of the $^{45}Ca^{2+}$ flux when compared with cell-free membrane values (Fig. 5B).

MRPC-1 cells grown in Ca^{2+}-containing medium exhibited no difference in $^{45}Ca^{2+}$ flux from the lower to the upper Transwell chamber when compared with cells in Ca^{2+}-depleted conditions (Fig. 6A). After 20 minutes of incubation, the cellular barrier tightness in Ca^{2+}-containing medium did not differ from that in the Ca^{2+}-depleted system. In the other direction, however, from the upper to the lower chamber, there was a difference in cellular ability to uphold the barrier function, the depletion of Ca^{2+} resulting in a significantly ($P < 0.01$) higher transcellular Ca^{2+} flux as seen after 10 minutes of incubation (Fig. 6B).

Porcine thyrocytes, which were assayed in the same system for comparison, exhibited a different behavior. In the presence of Ca^{2+} in the Transwell chambers, essentially no $^{45}Ca^{2+}$ passed through the thyrocyte monolayer grown on the membrane (Fig. 7). When depleted of Ca^{2+}, however, this barrier to Ca^{2+} fluxes was severely compromised. Already at the onset of the incubation, the barrier was disrupted in both directions ($P < 0.001$), and the difference between $^{45}Ca^{2+}$ fluxes in the Ca^{2+}-depleted system and in

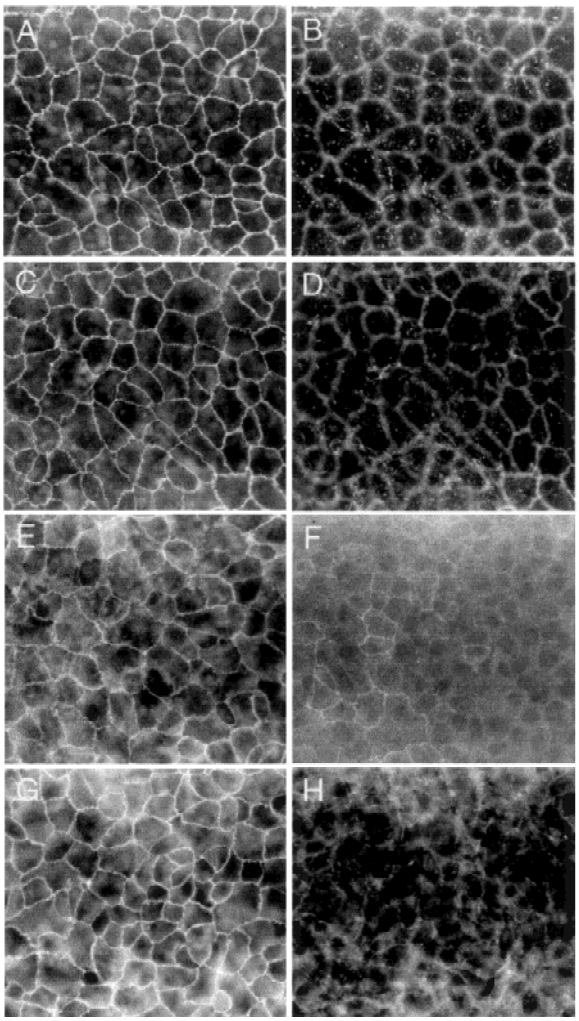

Fig. 3. Immunoreactivity of tight and adherens junction proteins in cultured MRPC-1 cells. (**A**) Immunoreactivity of ZO-1 in the superior cell layer appeared as thin homogenous lines outlining the cell borders. (**B**) In the basal cells, the homogenous immunoreactivity was strongly decreased and appeared as irregular dots. (**C**) E-cadherin also outlined the circumference of all cells in the upper cell layer. (**D**) In the basal cells, the immunoreactivity was essentially absent. With pan-cadherin antibodies, immunostaining appeared with a similar pattern and intensities in both the upper (**E**) and lower (not shown) cell layers. Although somewhat less regular than E-cadherin, the staining essentially outlined all cells. (**F**) Occludin immunoreactivity was weak and irregular. Within groups of cells in the upper layer, staining outlined the cellular circumference, whereas other groups of cells were unstained. (**G**) Immunostaining for β-catenin appeared as thin homogenous lines outlining the circumference of all upper layer cells. (**H**) Close to the basal part of these cells and below, the regular immunoreactivity was lost. ×40.

the Ca^{2+}-containing medium further increased throughout the 20-minute experiment, both in case of flux from the lower to the upper chamber ($P < 0.001$) (Fig. 7A) and from the upper to the lower one ($P < 0.01$) (Fig. 7B).

As shown above (Figs. 6, 7), MRPC-1 cells differed from thyrocytes in that a certain transcellular $^{45}Ca^{2+}$ flux occurred over the MRPC-1 cell layer on the Transwell membranes. The final experiment was performed to investigate whether this transcellular $^{45}Ca^{2+}$ transport was mediated by the cells and inhibitable. For this purpose, nifedipine, an inhibitor of Ca^{2+} channels of the L-type, was employed. After a 20-minute pretreatment with 5 μM nifedipine in the lower Transwell compartment, no difference in $^{45}Ca^{2+}$ fluxes from the lower to the upper compartment was evident between treated and untreated cells (Fig. 8A). When nifedipine was added to the upper chamber, however, the $^{45}Ca^{2+}$ transport from the upper to the lower compartment was essentially totally inhibited (Fig. 8B).

Discussion

The MRPC-1 cell line is an odontoblast-like cell line originally subcloned from the rat incisor pulp RPC-C2A cell line [8]. MRPC-1 cells form mineralized nodules *in vitro*, express dentin sialophosphoprotein (DSPP), collagen type I, high alkaline phosphatase activity [Marsh & Ritchie, unpublished], and shows the identical expression of NCX1 Na^+/Ca^{2+} exchanger isoforms as odontoblasts and osteoblastic cells [7, 9]. In the present study, we report that MRPC-1 cells form a bilayer of flattened cells separated by a thin collagenous matrix when cultured on filter, and that they exhibit morphological, biochemical and functional features of epithelial-like cells. When confluent on Transwell membranes, the MRPC-1 cells formed a low-resistance cell layer (<200 $\Omega \cdot cm^2$). This resistance was essentially fully established after 3 days in culture (Fig. 1). Therefore, our Transwell experiments were typically performed after 6 days in culture. In comparison, high-resistance epithelial cells, such as thyrocytes, may develop transcellular resistance values exceeding 6 $k\Omega \cdot cm^2$ [12, 13].

The results indicated a clear functional difference between the two MRPC-1 cell layers in culture. Distinct intercellular junctional complexes were primarily seen between cells in the superior layer, and this difference was also evident in the immunoreactivities for various junction-associated proteins (Fig. 3). The upper cell layer showed distinct circumferential cellular staining with ZO-1, E-cadherin, pan-cadherin, and β-catenin antibodies, similar to thyroid cells in monolayer [11, 14], whereas such a reactivity was essentially only seen with pan-cadherin antibodies in the lower MRPC-1 cell layer. Pan-cadherin antibodies are raised against a conserved sequence of N-cadherin and are often used as an overall cadherin detector. Of the four cell types, MRPC-1 showed the strongest immunostaining on westerns with both N-cadherin and pan-cadherin antibodies and with an identical electrophoretic migration (Fig. 4). This indicates that pan-cadherin immunoreactivity in MRCP-1 cells largely represented N-cadherin. In native odontoblasts *in situ*, earlier electron microscopic studies demonstrated morphologically distinguishable tight junctions between the distal, predentin-near, parts of odontoblasts [15–19]. In those studies, however, the circumcellular tight junction belt was reported to be more or less incomplete.

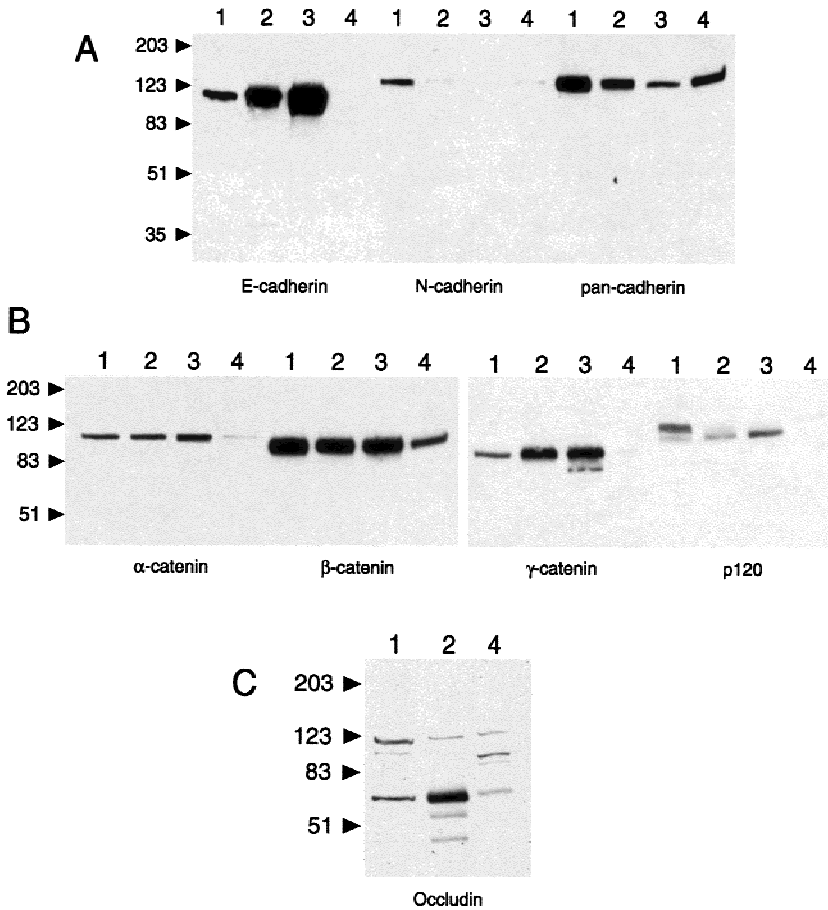

Fig. 4. Western blots of cadherins (**A**), catenins (**B**), and occludin (**C**). Lane 1: MRPC-1 cells; lane 2: MDKC kidney cells; lane 3: porcine thyrocytes; lane 4: MRC-5 fibroblasts. (**A**) Immunoblots for E-cadherin demonstrated a major band at 120 kDa in MRPC-1 cells, MDKC cells, and thyrocytes. The intensity was highest in thyrocytes. In MDCK cells a minor band with an apparent M_r of 38 kDa was also seen. MRC-5 fibroblasts showed no E-cadherin staining. N-cadherin was expressed as a single strong band at 134 kDa in MRPC-1 cells, whereas the expression was very weak in the other cells. Blotting with pan-cadherin antibodies resulted in a major band at 134 kDa in all cell types. The expression was strongest in the MRPC-1 cells. (**B**) α-catenin was expressed as a single band at 102 kDa in MRPC-1, MDKC, and thyrocytes but was only weakly discernible in MRC-5 fibroblasts. β-catenin was expressed as a major band at 92 kDa in all cell types with least intensity in MRC-5 cells. γ-catenin was expressed at 82 kDa in MRPC-1 cells, MDKC cells, and thyrocytes, with MRPC-1 cells being the weakest. In thyrocytes, a minor band with higher migration was also seen, whereas staining was barely discernible in MRC-5 fibroblasts. When antibodies to $p120^{cat}$-catenin were used, bands appeared both at 115 kDa and 100 kDa. Both bands were visible in MRPC-1 cells, the 115 kDa band clearly being the strongest. In MDKC cells and thyrocytes the 100 kDa band predominated, even though a faint staining could also be seen th the higher M_r. In fibroblasts the 115 kDa band was vaguely discernible. (**C**) Blotting with anti-occludin demonstrated a major band at 67 kDa that was weaker in MRPC-1 than in MDKC cells. MRC-5 fibroblasts expressed the band weakly. In addition to the 67 kDa band, a band with higher molecular weight, 116 kDa, appeared in all cell types.

The occurrence of junction-associated proteins in epithelial cells has been thoroughly examined, such as during tooth development [20–24] and in the thyroid follicular epithelium [10, 13, 25]. In cells of mesenchymal origin, those proteins have been less studied. In dental papilla cells of murine tooth germs, *e.g.,* β-catenin was discerned during the cap and bell stages [22], and ZO-1 has been found to be present at low levels in fibroblasts [26–28]. So far, no study has specifically addressed the expression of tight or adherens junction proteins in dentinogenically active odontoblasts.

Odontoblasts originate from the neural crest and are considered as ecto-mesenchymal in origin. A question is, therefore, if this in some way is reflected in the MRPC-1 cells, and in which way MRPC-1 cells would differ from fibroblasts and epithelial cells, respectively. Clear differences were actually shown by the expression of junction-associated proteins as demonstrated by western blots (Fig. 4). The two epithelial cell lines (MDCK cells and porcine thyrocytes) showed a strong expression of E-cadherin, whereas the MRC-5 fibroblasts were devoid of such an expression. E-cadherin is recognized as belonging to an epithelial phenotype, but it may be expressed in other cell types as well. We thus found that E-cadherin was expressed at an intermediate level in MRPC-1 cells. This is in contrast to osteoblastic cells [29, 30], which share common features with odontoblasts. It is an interesting observation that transfection of fibroblasts with a plasmid containing the E-cadherin gene caused a transdifferention into an epithelial phenotype [29], so it may be that MRPC-1 E-cadherin expression is related to the epithelial-like features of these cells *in vitro.* Of the cells analyzed, MRPC-1, showed the strongest N-cadherin expression, which is characteristically present in neural tissues. However, expression of N-cadherin has earlier been demonstrated in human osteoblasts [30] and osteoblastic cell lines [30, 31] *in vitro.* Likewise, N-cadherin but not E-cadherin was found in periodontal ligament cells forming mineralized nodules *in vitro* [32].

Another major difference from fibroblasts was that, except for β-catenin, catenin expressions were very low in

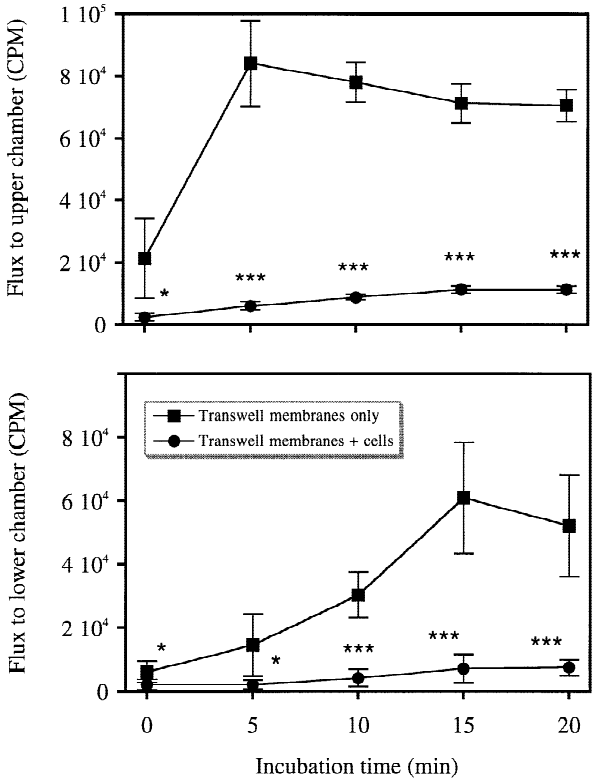

Fig. 5. MRPC-1 cells grown on Transwell membranes comprises a calcium ion flux barrier. $^{45}Ca^{2+}$ added to the lower compartment in cell-free Transwells easily diffused into the upper compartment (upper panel). When replaced with cell-covered Transwell membranes, the $^{45}Ca^{2+}$ flux was significantly hindered. After 20 minutes, cell-covered Transwell membranes exhibited a 16.3% $^{45}Ca^{2+}$ flux when compared with cell-free membranes ($P < 0.001$). Likewise, when added to the upper compartment in cell-free Transwells, $^{45}Ca^{2+}$ easily diffused into the lower compartment (lower panel), whereas $^{45}Ca^{2+}$ flux was significantly hindered by cell-covered membranes. After 20 minutes, cell-covered Transwell membranes exhibited 14.3% of the $^{45}Ca^{2+}$ flux when compared with cell-free membranes ($P < 0.001$).

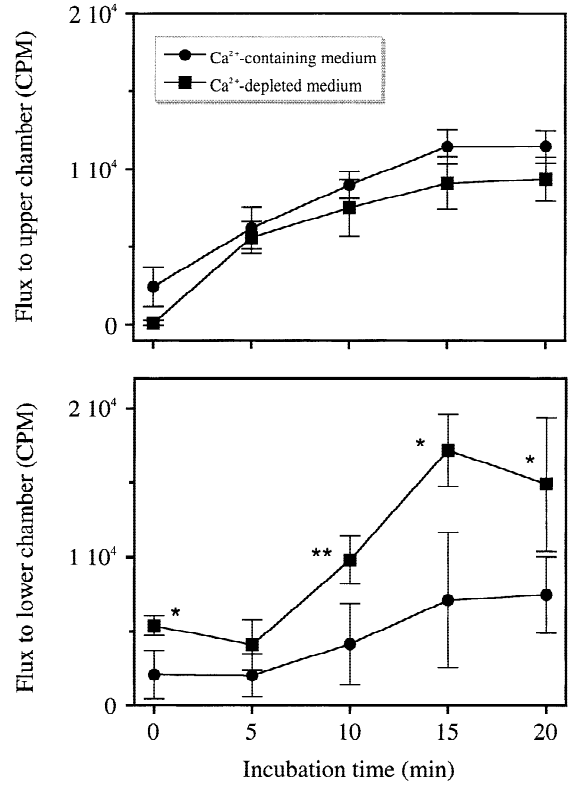

Fig. 6. MRPC-1 cells in Ca^{2+}-containing medium exhibited no difference in $^{45}Ca^{2+}$ flux from the lower to the upper Transwell compartment when compared to cells in Ca^{2+}-depleted medium in both chambers (upper panel). In contrast, when $^{45}Ca^{2+}$ flux was assayed in the other direction, from the upper to the lower compartment, the barrier function was compromised in Ca^{2+}-depleted medium (lower panel). $^{45}Ca^{2+}$ fluxes were significantly higher in Ca^{2+}-depleted medium ($P < 0.01$ at 10 minutes; $P < 0.05$ at 15 and 20 minutes of incubation).

MRC-5 fibroblasts. Like the two epithelial cell lines, MRPC-1 cells expressed both α- and γ-catenin (plakoglobin), the latter, however, at clearly lower levels than in the epithelial cells. A conspicuous finding was the high levels of $p120^{cat}$ expressed by MRPC-1 cells (Fig. 4B). MDCK cells and thyrocytes showed immunoreactivity on western blots with anti-$p120^{cat}$ antibodies as well, however at a lower apparent M_r. $p120^{cat}$ was originally characterized as a tyrosine kinase substrate implicated in both cell transformation and ligand-induced receptor signaling. Due to its structural similarity with β- and γ-catenins, primarily a number of Armadillo repeat motifs, it was eventually identified as a catenin [33], associating with both E-cadherin and N-cadherin [34]. Unlike β- and γ-catenins, however, $p120^{cat}$ does not seem to be linked to the cytoskeleton through α-catenin but binds to a different juxtamembrane domain on cadherins, and its functional significance is presently not understood. In mouse, $p120^{cat}$ is expressed as at least four isoforms (CAS1A/B and CAS2A/B) with CAS1A/B ≈115/112 kDa and CAS2A/B ≈96/100 kDa [33]. The epithelial MDCK cells have been shown to express mainly CAS2 isoforms [33], which agrees with our result. The intense expression by the MRPC-1 cells would correspond to one or both of the CAS 1 isoforms (Fig. 4B).

Occludin was strongly expressed in MDCK cells, less strongly in MRPC-1 cells, and sparsely in fibroblasts (Fig. 4C). Earlier results have, however, indicated an absence of occludin expression in fibroblasts, as revealed by negative western as well as northern blots [35]. Also the immunostaining of MRPC-1 cells in culture showed a scarce distribution of occludin (Fig. 3F). Occludin is known to contribute significantly to the formation of transepithelial resistance, and this may then be the reason for the definite but comparatively low transcellular resistance in MRPC-1 cells (Fig. 1).

The flux of $^{45}Ca^{2+}$ was significantly hindered between Transwell compartments in both directions by the epithelial-like MRPC-1 cell bilayer (Fig. 5). The MRPC-1 cells thus comprised a Ca^{2+} diffusion barrier, although some Ca^{2+} was found to pass across the MRPC-1 cell layer, in contrast to the tight barrier created by the epithelial thyrocytes (Fig. 7).

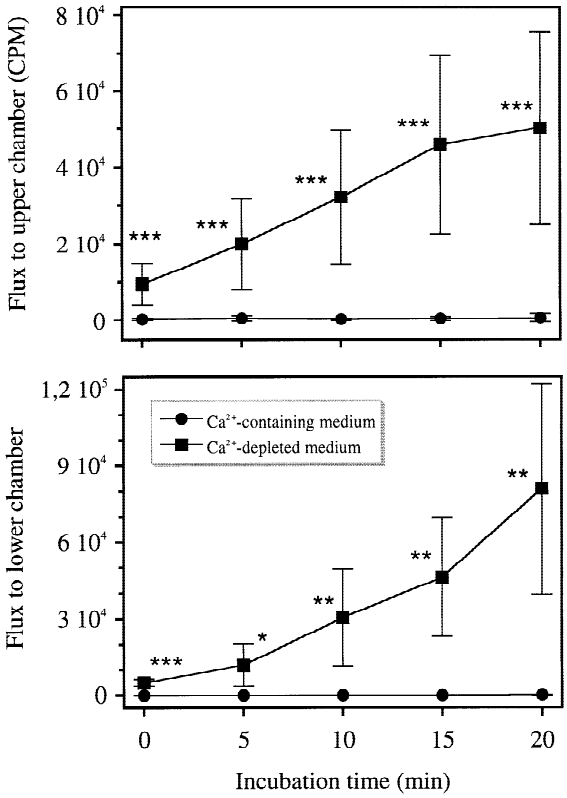

Fig. 7. In Ca^{2+}-containing medium, porcine thyrocytes constituted an essentially tight barrier for $^{45}Ca^{2+}$ fluxes, both from the lower to the upper Transwell compartment (upper panel) as well as from the upper to the lower compartment (lower panel). When media in both compartments were depleted of Ca^{2+}, this barrier was significantly compromised in both directions.

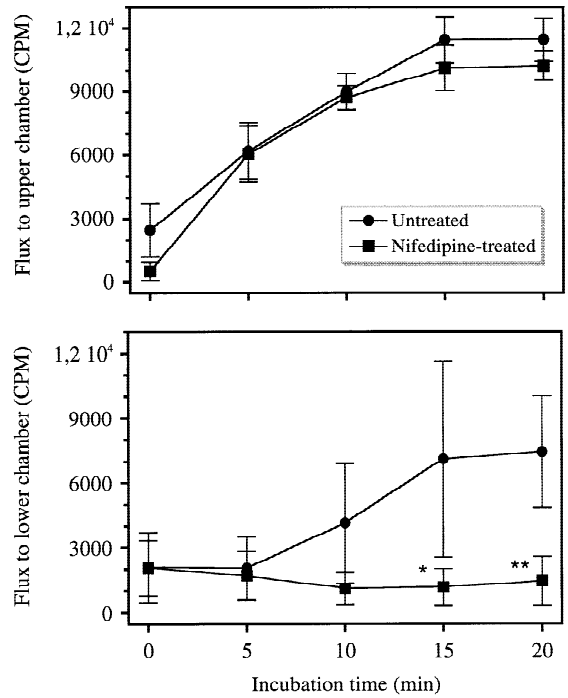

Fig. 8. No difference could be seen in $^{45}Ca^{2+}$ transport from the lower to the upper Transwell compartment whether or not cells were subjected to a 20 minute pretreatment with 5 μM nifedipine in the lower compartment (upper panel). When added to the upper compartment, however, nifedipine caused a total blocking of $^{45}Ca^{2+}$ transport from the upper to the lower compartment (lower panel). This difference in $^{45}Ca^{2+}$ flux was significantly different at 15 minutes ($P < 0.05$) and 20 minutes ($P < 0.01$).

The MRPC-1 diffusion barrier towards Ca^{2+} ions was dependent on calcium as well. $^{45}Ca^{2+}$ fluxes towards the lower chamber were significantly higher in Ca^{2+}-depleted medium (Fig. 6B), but such a difference was not found for $^{45}Ca^{2+}$ fluxes in the opposite direction (Fig. 6A), demonstrating a polarized Ca^{2+} dependence of the MRPC-1 barrier function. In contrast, thyrocytes, which grow in monolayer, exhibited a Ca^{2+}-sensitive barrier independent of the direction of $^{45}Ca^{2+}$ flux (Fig. 7). In the case of thyrocytes, the increase in ionic flux has been attributed to loss of function of the intercellular E-cadherin junctions upon Ca^{2+} depletion [25]. Whether this is the case also for MRPC-1 cells, which express E-cadherin (Figs. 3, 4), or some other Ca^{2+}-dependent adhesion mechanism is not yet known.

A difference between MRPC-1 cells and the epithelial thyrocytes was that while the barrier function *in vitro* of the latter towards Ca^{2+} was essentially total (Fig. 7), a certain amount of transcellular flow of $^{45}Ca^{2+}$ occurred continuously during the experiments with MRPC-1 cells (Figs. 5, 6, 8). When nifedipine, a dihydropyridine inhibitor of L-type Ca^{2+} channels in the plasma membrane, was added to MRPC-1 cells, only addition in the upper Transwell compartment had an inhibitory effect on transcellular $^{45}Ca^{2+}$ flux. $^{45}Ca^{2+}$ transport in the other direction was not inhibited (Fig. 8), thus giving additional evidence for a polarization of MRPC-1 cell function in culture. From the fact that it was possible to totally abolish transcellular fluxes in one direction follows that this transcellular flux, in fact, represents an active intracellular transport route, where Ca^{2+} uptake through voltage-gated L-type channels plays an essential role. We have demonstrated earlier that nifedipine inhibits uptake of Ca^{2+} in native rat incisor odontoblasts [6], and that plasma membrane-associated Ca^{2+} in these cells is decreased by nifedipine [36]. The finding that nifedipine administration to rats leads to a strongly decreased incorporation of $^{45}Ca^{2+}$ into the mineral phase of newly formed dentin, gave evidence for a cardinal role of L-type channels in Ca^{2+} transport across the odontoblast layer during dentinogenesis *in vivo* [4]. Further evidence for the importance of L-type channels during the formation of calcified tissues was given by the demonstration that nifidipine hampers osteogenesis *in vivo* [37].

In vivo, Ca^{2+} activities are significantly higher in the predentin compartment than in the dental pulp extracellular fluid during dentinogenesis [5]. Such a difference is dependent on the ability of the separating cell layer to constitute a diffusion barrier. The MRPC-1 cells displayed this property in culture, which may be ascribed to the junctional

proteins expressed by the MRPC-1 cells. The finding of a transcellular Ca^{2+} ion transport through the MRPC-1 cells which, as is the case for odontoblasts *in vivo*, occurs by a Ca^{2+} uptake through L-type channels gives additional evidence for the odontoblast-like features of the MRPC-1 cells. This, together with the findings of identical expression patterns of NCX1 Na^+/Ca^{2+} exchanger isoforms [7, 9] and Na^+/P_i cotransporters [38] as in native odontoblasts, makes it probable that MRPC-1 cells may serve a useful purpose for studying ion transport mechanisms of importance for the calcification process, specifically dentinogenesis.

Acknowledgments. The authors gratefully acknowledge the instructive help with cell cultures by Dr. Amel Gritli-Linde and the technical assistance of Ms. Therese Carlsson. The MRPC-1 cell line was originally developed by Drs. Mary E. Marsh and Helena H. Ritchie, which is hereby acknowledged. This study was supported by the Swedish Medical Research Council (grants 2789 and 537); the National Institutes of Health (grant DE11442 to HHR); the Swedish Dental Society; and the Sigge Persson & Alice Nyberg Research Fund.

References

1. Linde A, Goldberg M (1993) Dentinogenesis. Crit Rev Oral Biol Med 4:679–728
2. Linde A, Lundgren T (1995) From serum to the mineral phase. The role of the odontoblast in calcium transport and mineral formation. Int J Dev Biol 39:213–222
3. Bawden JW (1989) Calcium transport during mineralization. Anat Rec 224:226–233
4. Lundgren T, Linde A (1992) Calcium ion transport kinetics during dentinogenesis: effects of disrupting odontoblast cellular transport systems. Bone Miner 19:31–44
5. Lundgren T, Nannmark U, Linde A (1992) Calcium ion activity and pH in the odontoblast-predentin region: ion-selective microelectrode measurements. Calcif Tissue Int 50:134–136
6. Lundgren T, Linde A (1997) Voltage gated calcium channels and non-voltage gated calcium uptake pathways in the rat incisor odontoblast plasma membrane. Calcif Tissue Int 60:79–85
7. Lundquist P, Lundgren T, Gritli-Linde A, Linde A (2000) Na^+/Ca^{2+} exchanger isoforms of the rat odontoblast and osteoblast. Calcif Tissue Int 67:60–67
8. Kasugai S, Adachi M, Ogura H (1988) Establishment and characterization of a clonal cell line (RPC-C2A) from dental pulp of the rat incisor. Arch Oral Biol 33:887–891
9. Lundquist P, Lundgren T, Gritli-Linde A, Hanks CT, Ritchie HH, Linde A (2000) Sodium-calcium exchanger isoforms in odontoblast-like cell lines MDPC-23 and MMP4. In: Goldberg M, Boskey A, Robinson C (eds) Chemistry and biology of mineralized tissues. Am Acad Orthopaed Surg, Rosemont, IL, pp 233–236
10. Nilsson M, Björkman U, Ekholm R, Ericson LE (1990) Iodide transport in primary cultured thyroid follicle cells: evidence of a TSH-regulated channel mediating iodide efflux selectively across the apical domain of the plasma membrane. Eur J Cell Biol 52:270–281
11. Husmark J, Heldin NE, Nilsson M (1999) N-cadherin-mediated adhesion and aberrant catenin expression in anaplastic thyroid-carcinoma cell lines. Int J Cancer 83:692–699
12. Ericson LE, Nilsson M (1996) Effects of insulin-like growth factor I on growth, epithelial barrier and iodide transport in polarized pig thyrocyte monolayers. Eur J Endocrinol 135: 118–127
13. Nilsson M, Husmark J, Björkman U, Ericson LE (1998) Cytokines and thyroid epithelial integrity: interleukin-1 alpha induces dissociation of the junctional complex and paracellular leakage in filter-cultured human thyrocytes. J Clin Endocrinol Metab 83:945–952
14. Nilsson M, Ericson LE (1995) Effects of epidermal growth factor and phorbol ester on thyroid epithelial integrity. Exp Cell Res 219:626–639
15. Sasaki T, Nakagawa K, Higashi S (1982) Ultrastructure of odontoblasts in kitten tooth germs as revealed by freeze-fracture. Arch Oral Biol 27:897–904
16. Iguchi Y, Yamamura T, Ichikawa T, Hashimoto S, Horiuchi T, Shimono M (1984) Intercellular junctions in odontoblasts of the rat incisor studied with freeze-fracture. Arch Oral Biol 29:487–497
17. Callé A (1985) Intercellular junctions between human odontoblasts. A freeze-fracture study after demineralization. Acta Anat 122:138–144
18. Callé A, Magloire H, Joffre A (1985) Intercellular junctions in human tooth-pulp cells in culture in vitro revealed by freeze-fracture, lanthanum impregnation and filipin treatment. Arch Oral Biol 30:283–289
19. Arana-Chaves VE, Katchburian E (1997) Development of tight junctions between odontoblasts in early dentinogenesis as revealed by freeze-fracture. Anat Rec 248:332–338
20. Lüning C, Rass A, Rozell B, Wroblewski J, Öbrink B (1994) Expression of E-cadherin during craniofacial development. J Craniofac Genet Dev Biol 14:207–216
21. Palacios J, Benito N, Berraquero R, Pizarro A, Cano A, Gamallo C (1995) Differential spatiotemporal expression of E- and P-cadherin during mouse tooth development. Int J Dev Biol 39:663–666
22. Fausser JL, Schlepp O, Aberdam D, Meneguzzi G, Ruch JV, Lesot H (1998) Localization of antigens associated with adherens junctions, desmosomes, and hemidesmosomes during murine molar morphogenesis. Differentiation 63:1–11
23. Obara N, Suzuki Y, Nagai Y, Takeda M (1998) Expression of E- and P-cadherin during tooth morphogenesis and cytodifferentiation of ameloblasts. Anat Embryol (Berlin) 197:469–475
24. Obara N, Suzuki Y, Nagai Y, Takeda M (1999) Immunofluorescence detection of cadherins in mouse tooth germs during root development. Arch Oral Biol 44:415–421
25. Nilsson M (1991) Integrity of the occluding barrier in high-resistant thyroid follicular epithelium in culture. I. Dependence of extracellular Ca^{2+} is polarized. Eur J Cell Biol 56:295–307
26. Howarth AG, Hughes MR, Stevenson BR (1992) Detection of the tight junction-associated protein ZO-1 in astrocytes and other nonepithelial cell types. Am J Physiol 262:C461–469
27. Itoh M, Nagafuchi A, Yonemura S, Kitani-Yasuda T, Tsukita S, Tsukita S (1993) The 220-kD protein colocalizing with cadherins in non-epithelial cells is identical to ZO-1, a tight junction-associated protein in epithelial cells: cDNA cloning and immunoelectron microscopy. J Cell Biol 121:491–502
28. Yonemura S, Itoh M, Nagafuchi A, Tsukita S (1995) Cell-to-cell adherens junction formation and actin filament organization: similarities and differences between non-polarized fibroblasts and polarized epithelial cells. J Cell Sci 108:127–142
29. Vanderburg CR, Hay ED (1996) E-cadherin transforms embryonic corneal fibroblasts to stratified epithelium with desmosomes. Acta Anat 157:87–104
30. Cheng SL, Lecanda F, Davidson MK, Warlow PM, Zhang SF, Zhang L, Suzuki S, St. John T, Civitelli R (1998) Human osteoblasts express a reportoire of cadherins, which are critical for BMP-2-induced osteogenic differentiation. J Bone Miner Res 13:633–644
31. Tsutsumimoto T, Kawasaki S, Ebara S, Takaoka K (1999) TNF-α and IL-1β suppress N-cadherin expression in MC3T3-E1 cells. J Bone Miner Res 14:1751–1760

32. Lin WL, Chien HH, Cho MI (1999) N-cadherin expression during periodontal ligament cell differentiation in vitro. J Periodontol 70:1039–1045
33. Reynolds AB, Daniel J, McCrea PD, Wheelock MJ, Wu J, Zhang Z (1994) Identification of a new catenin: the tyrosine kinase substrate $p120^{cas}$ associates with E-cadherin complexes. Mol Cell Biol 14:8333–8342
34. Reynolds AB, Daniel JM, Mo YY, Wu J, Zhang Z (1996) The novel catenin $p120^{cas}$ binds classical cadherins and induces an unusual morphological phenotype in NIH3T3 fibroblasts. Exp Cell Res 225:328–337
35. Saitou M, Ando-Akatsuka Y, Itoh M, Furuse M, Inazawa J, Fujimoto K, Tsukita S (1997) Mammalian occludin in epithelial cells: its expression and subcellular distribution. Eur J Cell Biol. 73:222–231
36. Lundgren T, Linde A (1998) Modulation of rat incisor odontoblast plasma membrane-associated Ca^{2+} with nifedipine. Biochim Biophys Acta 1373:341–346
37. Duriez J, Flautre B, Blary MC, Hardouin P (1993) Effects of the calcium channel blocker nifedipine on epiphyseal growth plate and bone turnover: A study in rabbit. Calcif Tissue Int 52:120–124
38. Lundquist P, Lundgren T, Linde A, (2001) Expression and activity of Na^{+}-P_i cotransporters in rat odontoblasts, MRPC-1 odontoblast-like and UMR-106.01 osteoblast-like cells. J Bone Min Res (submitted)